PCCP

Accepted Manuscript

ROYAL SOCIETY OF CHEMISTRY

www.rsc.org/pccp

Journal Name

RSCPublishing

COMMUNICATION

Why do the $[PhSiO_{1.5}]_{8,10,12}$ cages self-brominate primarily in the ortho position? Modeling reveals a strong cage influence on the mechanism.

Cite this: DOI: 10.1039/x0xx00000x

Received 00th January 2012,
Accepted 00th January 2012

DOI: 10.1039/x0xx00000x

www.rsc.org/

M. Bahrami,[a] H. Hashemi,[a] X. Ma,[a] J. Kieffer,[a*] R.M. Laine[a,b*]

$(PhSiO_{1.5})_{8,10,12}$ cages are bulky, electron withdrawing like CF_3; yet self-brominate (60 °C), favoring ortho substitution: PhT_8 (≈ 85 %), PhT_{10} (≈ 75 %) and PhT_{12} (60 %). First-principles calculations suggest bromination initiates when Br_2 is "trapped" via H-bonding to ortho–H's, followed by polarization via strong interactions with *cage faces*, possibly cage LUMOs.

Aromatic halogenation reactions are among the oldest known organic reactions.[1-12] There are multiple reviews on various aspects of aromatic halogenation.[9-12] Multiple kinetic and mechanistic studies have been reported as well as extensive studies on the catalysis of these reactions. In general it is well recognized that monosubstituted phenyl rings, where the substituent is electron donating, usually halogenate at either the ortho or para positions. Likewise when the substituent is electron-withdrawing, substitution occurs preferentially in the meta position. These results have long been explained as an effect of conjugation in the transition state that stabilizes the cationic intermediate in the case of electron donating substituents and does exactly the opposite for electron accepting substituents.

Although halogenations usually require catalysts to promote electrophilic substitution there are examples where no catalysts are needed to effect efficient and multiple halogenation as seen in reactions of phenols or anilines.[13,14] In contrast, efforts to halogenate aromatic rings with highly electron withdrawing groups such as nitro or CF_3- require the use of catalysts such as FeX_3 and relatively high temperatures. For example, nitrobenzene is usually meta brominated using catalytic amounts of $FeBr_3$ at ≥ 140 °C. Indeed, as expected $AlCl_3$ catalyzed Friedel-Crafts acylation and sulfonation provide phenyl cages where meta selectivity is > 80 % as the $SiO_{1.5}$ corner offers electron withdrawing properties akin to $–CF_3$.[15-18]

In contrast to traditional aromatic bromination, we have reported that uncatalyzed bromination of $[PhSiO_{1.5}]_8$ in refluxing dichloromethane leads, after recrystallization to $[o\text{-}BrPhSiO_{1.5}]_8$, where ortho bromination dominates, 85 %.[16] This result is supported by both single crystal x-ray diffractometry and selective Si-C bond cleavage with F^-/H_2O_2. In contrast to this result, iodination of $[PhSiO_{1.5}]_{8,10,12}$ with ICl at -40 °C leads almost exclusively (> 90 % selectivity) to the para products, $[p\text{-}IPhSiO_{1.5}]_{8,10,12}$ as also supported by single crystal X-ray diffraction.[16]

In this report, we extend bromination selectivity studies to the larger cages $[PhSiO_{1.5}]_{10,12}$ finding similar ortho selectivity and through modelling studies find a very novel mechanism wherein the incoming bromine interacts with a cage LUMO coincident with hydrogen bonding to the ortho hydrogens of the phenyl groups. The overall reaction mechanism can be likened to a *Venus fly trap*.

Our ability to extend these studies was enabled by the discovery of much improved routes to the larger cages (see experimental in ESI. Basically all of the cages will brominate without catalyst in refluxing dichloromethane with high selectivity to monobromination per phenyl as determined by mass spectral analysis and oxidative cleavage using F^-/H_2O_2 to produce the bromophenol compounds, see Table **S1**. Note that $PhSiCl_3$ selectivity for ortho-bromination is only 5 % by comparison.[19] Table **S2** records the ipso carbon ^{13}C for the starting materials and products and is provided to demonstrate that the cage offers properties akin to CF_3 substitution,[20] which should drive the formation of the meta product rather than the ortho or para product.

A number of theoretical studies have now been published that describe HOMO-LUMO interactions in a wide variety of silsesquioxane cages.[21-28] Of particular interest to the current work is the work of Hagelburg et al and Mabry, Bowers et al., who attempted to identify transition states that lead to F^- incorporation into T_8 cages.[27,28] Their modeling studies were motivated by the work of Bassindale et al,[29,30] who reported the first syntheses of cage encapsulated F^- and suggested that the cage's ability to stabilize this encapsulated anion

without being greatly affected electronically may arise because the F^- resides within the cage LUMO.

Thus, the modeling studies of Hagelburg et al and Mabry, Bowers et al attempt to explain this stabilization as well as the mechanism(s) whereby F^- approaches the cage and becomes incorporated. The majority of the cited theoretical studies find that the cage HOMO resides on the oxygen lone electron pairs. In addition, the majority of these studies find that the LUMO sits in the center of the cage and is quite electrophilic as suspected by Bassindale et al. The only discussion of HOMO-LUMO energies of aromatic silsesquioxanes is that of Mabry, Bowers et al, who find that both the HOMO and LUMO energies they calculate are associated with the aromatic rings only. They also report that for $CF_3(CH_2)_2$ groups on T_8 cages the frontier orbitals are located on these groups rather than on the cage.

The electronic structure and properties of T_8, T_{10} and T_{12} molecules, i.e., hydrogen terminated polyhedral oligomeric silsesquioxane (SQ) cages are first studied using local orbitals in a full potential representation, in the framework of density functional theory and the generalized gradient approximation methods as implemented in Gaussian03.[30] B3LYP as the exchange-correlation functional has been chosen.[31] The sturctures have been optimized without any symmetry (maximum degrees of freedom) using 6-31G* contracted Gaussian basis set with polarization functions.[32,33]

Because of the important role of the long-range interactions in Br_2 adsorbtion on the T_8,T_{10}, and T_{12} cages, the initial adsorption calculations have been verified with the Vienna ab Initio Simulation Package (VASP),[34,35] with added van der Waals long range interactions.[36] Projector-augmented-wave (PAW) potentials[37] have been used to mimic the ionic cores, while the generalized gradient approximation (GGA) in the Perdew Burke Ernzerh[38,39] of (PBE) flavor has been employed for the exchange and correlation functional. A conjugate gradient algorithm has been used to relax the ions and the lattice vectors. Ionic and electronic relaxation has been performed by applying a convergence criteria of 10^{-2} eV/Å and 10^{-4} eV, respectively. Convergence with respect to the plane wave cutoff has been checked carefully.

NMR simulated spectra were generated using ChemBioDraw Ultra Version 12.0.3.1216 (cambridgesoft.com) and used for comparative purposes with experimentally determined data.

In our efforts to develop an understanding of the bromination process, we first modeled the HOMO-LUMO structures (see experimental section) of the parent cages where R = H rather than phenyl generating the Figure **1** iso-electron density maps.[31-39] The HOMO energies of T_8, T_{10} and T_{12}, as indicated in Table **S3** are -8.48 eV, -8.62 and -8.62, respectively. The LUMO energies are 0.42 eV, 0.46 eV, 0.50 eV, respectively. The HOMO and LUMO gaps are 8.90, 9.08, and 9.13 eV, respectively. Note that these values are solely for the R = H system. They are very similar to calculations and absorption band modeling made by Shen et al[26] for T_8 and T_{10} R = Me. The first studies in this area by Vprek and Marsmann et al[23] modeled the band gaps for the $[RSiO_{1.5}]_8$ compounds where R = Me, Et, Pr…Dec. estimating the band gap to be ≈ 6 eV. However, this group also measured the optical absorptions and emissions of these compounds determining that the average band gap is closer to 4 eV. The HOMOs originate from the atomic orbitals (AOs) of lone-pair electrons on oxygen atoms.

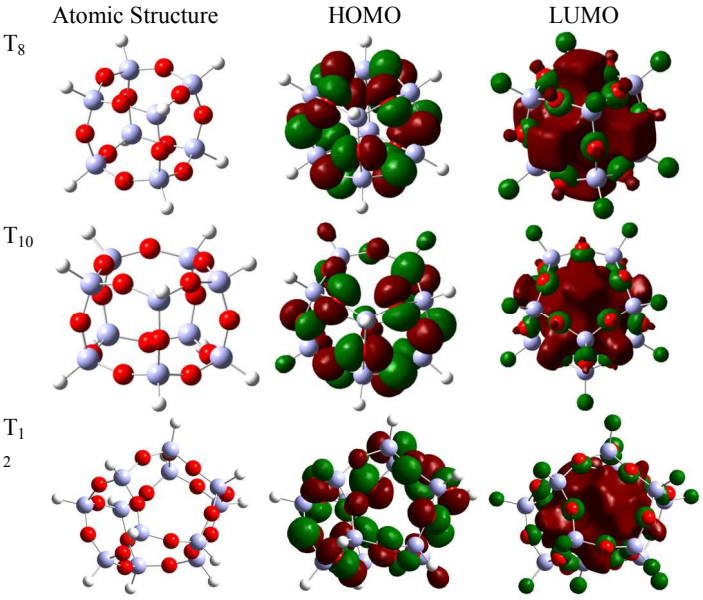

Figure 1. Molecular structures and electron density isocontours of $[PhSiO_{1.5}]_{8,10,12}$ cages. The left column shows a 3D view of the optimized structures with H (white), O (red) and Si (gray). HOMOs are shown in the middle and the right column presents LUMOs.

The LUMOs materialize prominently in the centers of the SQ cages with some extension through the faces of the cages. Our calculations suggest that the HOMO-LUMO gap increases slightly but steadily from T_8 to T_{12}, probably because of subtle differences in the way the different cage geometries can accommodate the bonding orbitals between cage constituents.

The next step was to model the approach and adsorption of Br_2 with all of the SQ cage surfaces. Total-energy calculations were used to elucidate the initial adsorption energetics of Br_2 on the HT_8, HT_{10} and HT_{12} molecules. The energetics were mapped using an adsorbed Br_2 to probe all symmetrically distinct sites and relative orientations. All attempts converged to the same fully relaxed configuration shown in Figures **2b** and **c**.

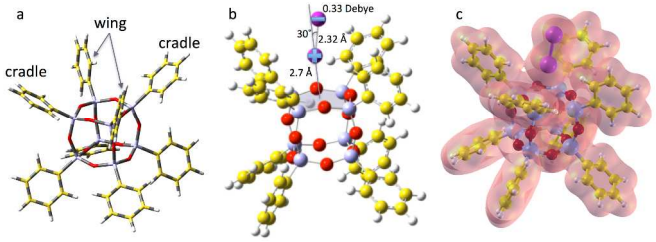

Figure 2. Br_2 absorption centrally above the T_8 cage face is preferred. The face has two phenyls oriented with hydrogens in (wing) and two turned at 90° (cradle, a). Br_2 is stabilized in this configuration due to hydrogen bonding between the closer Br atom and the two ortho-hydrogen atoms on the wing-oriented phenyl rings. Polarization occurs coincidentally as the Br_2 interacts with the T_8 face (b). The contour maps of electron density are presented in (c). Carbon atoms are shown by gray, oxygen by red, silicon by purple, bromine by brown, and hydrogen by white. Two orientations are shown for clarity.

While phenyl rings can easily pivot about the Si-C bond that connects them to the cube, we single out two characteristic orientations to serve as geometric descriptors to explain the SQ-Br_2 interactions: (i) the cradle orientation in which the normal vectors

emanating from the center of two rings attached to silicon atoms on opposite sides of a face diagonal intersect above the center of this face (left and right ring on the top face of the cube shown in Figure **2a**, and (ii) the wing orientation in which these normal vectors are approximately parallel to each other, as well as the face plane (front and back rings). In the latter orientation, the H atoms reach over the cage face.

We can identify two significant contributions to the SQ-Br_2 interactions. First, the Br_2 molecule gets trapped centrally above the cage face, where it is stabilized predominantly due to hydrogen bonding between the closer Br atom and the two H-atoms in ortho-positions of the wing-oriented phenyl rings. The closer Br atom is exactly equidistant to the two ortho-hydrogen atoms on opposing phenyl rings, when these rotate to a near perfect wing orientation. In a sense, this trapping mechanism *is reminiscent of that of a Venus flytrap*, except that the phenyl rings pivot rather than tilt. Both H-Br distances are 2.8 Å, which is the shortest to any atom in the SQ-phenyl complex; the nearest oxygen is 0.5 Å farther away.

Once in this position, the bromine molecule becomes polarized due to Coulomb interactions with the oxygen atoms on the face of the cage, which carry a negative charge of 0.65 electron units each. Electron density is shifted from the closer to the farther bromine atom and a small amount of charge is transferred to the cage complex via the ortho-H atoms, resulting in a net dipole moment of 0.33 Debye for Br_2. The combined effects of electrostatic repulsion between bromine and oxygen, the strong attraction between hydrogen and bromine, and the slight asymmetry in the Br_2 positioning, i.e., the 30° angle Br_2 assumes with respect to the cage face normal, eventually causes one H-Br bond to prevail, resulting in the formation of HBr, while the second bromine atom assumes the ortho-position on the phenyl ring.

The electrophilic LUMO of the SQ-phenyl complex, which extends beyond the cage, could potentially facilitate this process by offering energetically favorable electron transfer pathways.

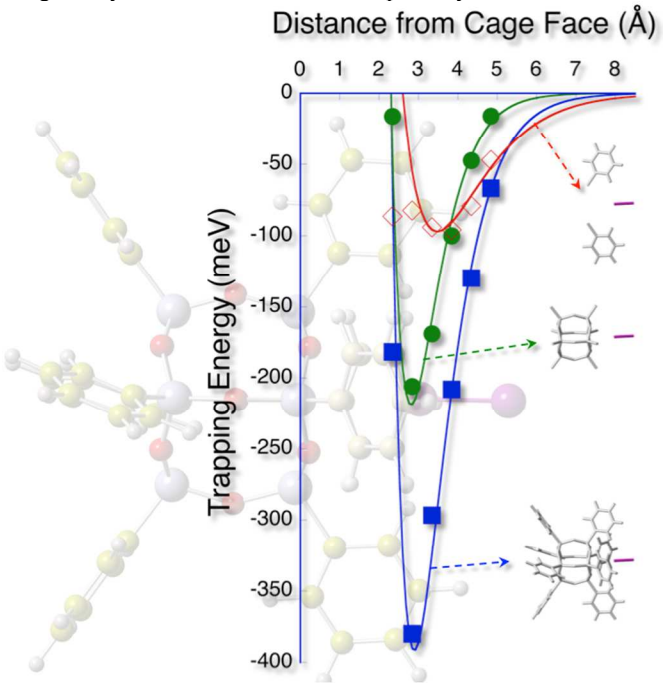

Figure 3. Energy gained on trapping the Br_2 molecule as a function of the distance from the cage face. The blue squares represent energies associated with trapping Br_2 near a phenyl-functionalized SQ cube, as is done here. For comparison, the energies associated with stabilizing Br_2 near a T8 cube (green circles) and between two benzene rings (red diamonds) are also plotted. For the latter calculations the cube and rings remained in the exact same positions as for the phenyl-functionalized SQ molecule. The distance axis is superimposed to scale on a schematic of the SQ-phenyl complex and fit lines are provided to guide the eye.

Figure **3** shows the energetics associated with this trapping mechanism. Accordingly, the bonding energy associated with the trapped state near the SQ-phenyl complex is 380 meV. By comparison, trapping of Br_2 by two benzene rings alone, held in positions equivalent to those attached to the SQ cube, yields about 95 meV and trapping by a non-functionalized SQ cube about 210 meV. *These two quantities do not add up to 380 eV, which can be attributed to the significant charge redistribution between phenyl rings and the SQ that occurs in the complex*. One consequence of this trapping mechanism is that, being localized within the complex, the energy gained is transformed into significant vibrational motion of phenyl rings especially, which can contribute towards overcoming the activation energy for the bond exchange.

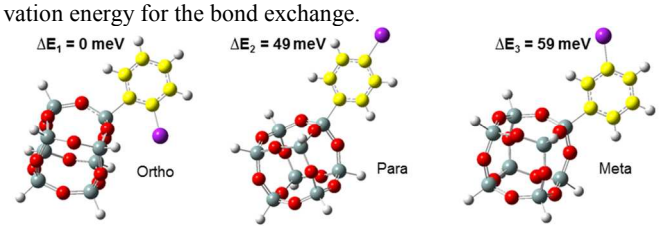

Figure 4. The relative stabilities of Br substitution at ortho, para or meta sites were also calculated in order to study the bromination mechanism of T_8 cage.

A final set of calculations was done to compare the stabilities of Br at the various positions on the phenyl ring leading to the Figure **4**, results. As seen, ortho bromo substitution is greatly favored energetically over para with meta being the least favored, which contrasts greatly with bromination of $PhSiCl_3$ where ortho is only 5 % of the product.[26] These calculations were done at absolute zero, and the resulting energetics are also given in Figure **4**. Applying Boltzmann statistics to estimate the relative population density of the different substitution types based on the calculated energy differences yields that, at ambient temperature, the ortho type is about four times more likely than the other two combined, which is close to the experimentally observed selectivity of 85%. The significantly higher stabilization of the ortho derivative (Figure **4**) compared with the para or meta positions may suggest further participation of the LUMO in the transition state that leads to aromatic substitution.

The reason for the observed selectivity can be ascribed most reasonably in terms of cage structure. Thus, the angle between phenyl groups in the T_8 cage is 90 °; whereas that for the T_{10} cage is 72° and if the T_{12} cage were fully symmetric, then the angle would be 60 °. Thus, one can easily argue that Br_2 adsorption would require relatively easy approach to cage faces. As the cages get bigger the separation between phenyl groups becomes smaller and as a consequence the approach of Br_2 becomes more sterically hindered leading to a lower proportion of ortho bromination of the T_{12} cage than our calculations might suggest. However, the proportion of ortho bromination at 60 % is still much greater than the 5 % found for bromination of $PhSiCl_3$ to give these results some perspective. This difference in proximity also has a remarkable effect on the emission behavior of these cages as we will report elsewhere (see experimental).[40-44]

Conclusions

In the above work, we first determined the bromination selectivity of the larger cages $[PhSiO_{1.5}]_{10,12}$ both experimentally and through theoretical modeling. We determined that bromination occurs via an unusual combination of hydrogen bonding to the ortho hydrogens of the phenyl groups coupled with an electronic interaction that stabilizes the transition state with the cage face by some 380 meV perhaps through LUMO interactions that create a partial dipole in the Br_2 leading to selective ortho bromination. Basically all three cages are non-innocent. They drive ortho selectivity by a combination of hydrogen bonding but more importantly through strong interactions of the cage with the incoming Br_2. These results may have implications for the chemical and physical properties of other hybrid cages and also for the chemistries of silica surfaces.

We suspect that a similar process works with ICl that causes the related selective para iodination and are in the process of conducting extensive modeling studies to this effect.[41-44]

Notes and references

[a]Dept of Mater. Sci. & Eng, Univ. of Michigan, Ann Arbor, MI 48109
[b]Macromolecular Sci. & Eng., Univ. of Michigan, Ann Arbor, MI 48109
[c] Address here.

†This work was supported by as part of the Center for Solar and Thermal Energy Conversion (CSTEC), an Energy Frontier Research Center funded by the U.S. Department of Energy (DOE), Office of Science, Basic Energy Sciences (BES), under Award # DE-SC0000957

Electronic Supplementary Information (ESI) available: [Experimental section, Tables 1-4]. See DOI: 10.1039/c000000x/

1. A. I. Vogel, Practical Organic Chemistry, *Chapter 4*., Halogenation of Aromatic Hydrocarbons.
2. S. N. Ege, "Organic chemistry," *Chapter 20*, The chemistry of aromatic compounds, Aromatic substitution reactions.
3. J. D. Hepworth, M. J. Waring, D. R. Waring, "Aromatic chemistry," *Chapter 9*. Aromatic halogen compounds.
4. F. Carey, "Advanced organic chemistry," *chapter 9*, aromatic substitution.
5. E. Berliner, *J. Am. Chem. Soc.,* 1960, **82**, 757–758.
6. J. S. Reese, *Chem. Rev*., 1934, **14**, 55–102.
7. C. C. Price, *Chem. Rev.,* 1941, **29**, 37–67.
8. L. N. Ferguson, *Chem. Rev.,* 1952, **50**, 47–67.
9. J. Pavlinac, M. Zupan, K. K. Laali, S. Stavber, *Tetrahedron,* 2009, **65**, 5625–5662.
10. D. E. Chumakov, A. V. Khoroshutin, A. V. Anisimov, K. I. Kobrakov, *Chem. Heterocyclic Cmpds,* 2009, **45**, 259-283.
11. R. O. C. Norman, R. Taylor, Electrophilic substitution in benzenoid compounds Elsevier N.Y., N.Y. 1965
12. P. Ratnasamy, A. P. Singh, S. Sharma, *Applied Catalysis A: General* 1996, **135**, 25-55.
13. E. Grovenstein, N. S. Aprahamian, C. J. Bryan, N. S. Gnanapragasam, D. C. Kilby, J. M. McKelvey, R. J. Sullivan, *J. Am. Chem. Soc*., 1973, **95**, 4261–4270.
14. L. Kumar, T. Mahajan, D. D. Agarwal, *Ind. Eng. Chem. Res.*, 2012, **51**, 2227–2234.
15. F.J. Feher, T.A. Budzichowski, *J. Organometallic Chem.*, 1989, **379**, 33-40.
16. a. R. M. Laine, M. F. Roll, *Macromolecules*, 2011, **44**, 1073-1109 and references therein. b. M. F. Roll, P. Mathur, K. Takahashi, J. W. Kampf, R. M. Laine, *J. Mater. Chem.*, 2011, **21**, 11167-11176. c. J. C. Furgal, T. Goodson III, R. M. Laine, "Synthesis and Experimental/Computational Reaction Analysis of Rare $D5_h$ Symmetric Decaphenyl Silsesquioxane (T_{10}) and Larger Cages by Fluoride Catalyzed Rearrangement of $[PhSiO_{1.5}]_n$ and Phenyltriethoxysilane" to be submitted.
17. C.M. Brick, Tamaki, R.; Kim, S.-G.; Asuncion, M.Z.; Roll, M.; Nemoto, T.; Ouchi, Y.; Chujo Y.; Laine, R.M. "Spherical, Polyfunctional Molecules Using Poly(bromophenylsil-sesquioxane)s as Nanoconstruction Sites," *Macromolecules,* 2005, **38**, 4655-4660.
18. Z. Li, R. Yang. J. Appl. Polymer Sci. **2014**, DOI: 10.1002/app.40892.
19. Private Communication, Dr. S. Sulaiman, Gelest Inc. Gelest Product SIB1903.0
20. R. A. Newmark, J. R. Hill, *Org. Mag. Res.* 1977, **9**, 589-592.
21. A. G. Calzaferri, R. Hoffmann, *J. Chem. Soc. Dalton Trans*. 1991**,** 917-928. b. G. Calzaferri, in Tailor-made Silicon-Oxygen Compounds, from molecules to materials, R. Corriu and P. Jutzi eds. Publ. Friedr. Vieweg & Sohn mbH, Braunshweig/Weisbaden, Germany **1996**. pp. 149-169.
22. Y. Chen, K. S. Schneider, M. Banaszak Holl, B. G. Orr, *Phys. Rev. B*, 2004, **70**, 85402.
23. a. C. Ossadnik, S. Veprek, H. C. Marsmann, E. Rikowski, *Monat. für Chem*. 1999, **130**, 55-68. b. D. Azinovic, J. Cai, C. Eggs, H. Konig, H. C. Marsmann, S. Veprek, *J. Luminescence*, 2002, **97**, 40-50.
24. a. H-C. Li, C-Y. Lee, C. McCabe, A. Striolo, M. Neurock, *J. Phys. Chem. A* 2007, **111**, 3577-3584. b. A. Striolo, C. McCabe, P. T. Cummings, *J. Phys. Chem. B* 2005, **109**, 14300-14307.
25. P. Cummings, S. Glotzer, J. Kieffer, C. McCabe, M. Neurock, *J. Comp. Theor. Nanosci.*, 2004, **1**, 265-279.
26. J. Shen, W. D. Cheng, D. S. Wu, X. D. Li, Y. Z. Lan, H. Zhang, Y. J. Gong, F. F. Li, S. P. Huang, *J. Chem. Phys*. 2005, **122**, 204709.
27. S. E. Anderson, D. J. Bodzin, T. S. Haddad, J. A. Boatz, J. M. Mabry, C. Mitchell, M. T. Bowers, *Chem. Mater.* 2008, **20**, 4299-4309.
28. S. S. Park, C. Xiao, F. Hagelberg, D. Hossain, C.U. Pittman, Jr., S. Saebo, *J. Phys. Chem. A* 2004, **108**, 11260-11272.
29. A. R. Bassindale, M. Pourny, P. G. Taylor, M. B. Hursthouse, M. E. Light, *Angew. Chem. Inter. Ed*. 2003, **42**, 3488-3490.
30. A. R. Bassindale, D. J. Parker, M. Pourny, P. G. Taylor, P. N. Horton, M. B. Hursthouse, *Organometallics* 2004, **23**, 4400-4405.
31. Gaussian 03, Revision C.02, M. J. Frisch, G. W. Trucks, H. B. Schlegel, G. E. Scuseria, M. A. Robb, J. R. Cheeseman, J. A. Montgomery, Jr. , T. Vreven, K. N. Kudin, J. C. Burant, J. M. Millam, S. S. Iyengar, J. Tomasi, V. Barone, B. Mennucci,M. Cossi, G. Scalmani, N. Rega, G. A. Petersson, H. Nakatsuji, M. Hada, M. Ehara, K. Toyota, R. Fukuda, J. Hasegawa, M. Ishida, T. Nakajima, Y. Honda, O. Kitao, H. Nakai, M. Klene, X. Li, J. E. Knox, H. P. Hratchian, J. B. Cross, V. Bakken, C. Adamo, J. Jaramillo, R. Gomperts, R. E. Stratmann, O. Yazyev, A. J. Austin, R. Cammi, C. Pomelli, J. W. Ochterski, P. Y. Ayala, K. Morokuma, G. A. Voth, P. Salvador, J. J. Dannenberg, V. G. Zakrzewski, S. Dapprich, A. D. Daniels, M. C. Strain, O. Farkas, D. K. Malick, A. D. Rabuck, K. Raghavachari, J. B. Foresman, J. V. Ortiz, Q. Cui , A. G. Baboul, S. Clifford, J. Cioslowski, B. B. Stefanov, G. Liu, A. Liashenko, P. Piskorz, I. Komaromi, R. L. Martin, D. J. Fox, T. Keith, M. A. Al-Laham, C. Y. Peng, A. Nanayakkara, M. Challacombe, P. M. W. Gill, B. Johnson, W. Chen, M. W. Wong, C. Gonzalez, J. A. Pople, Gaussian, Inc. , Wallingford CT, **2004**.
32. A. D. Becke, *Chem. Phys*. 1993, **98**, 5648–5652.
33. W. J. Hehre, R. Ditchfie, J. A. Pople, *J. Chem. Phys*. 1972, **56**, 2257–2261.
34. M. M. Franc, W. J. Pietro, W. J. Hehre, J. S. Binkley, M. S. Gordon, D. J. Defrees, J. A. Pople, *J. Chem. Phys*., 1982, *77*, 3654–3665.
35. G. Kresse, J. Hafner, *Phys. Rev. B* 1993, **48**, 13115-13118.
36. G. Kresse, J. Furthmüller, *Phys. Rev. B* 1996, **54**, 11169.
37. J. Klimeš, D. R. Bowler, A. Michaelides, *Phys. Rev. B* 2011, **83**, 195131(1)-195131(13).
38. G. Kresse, D. Joubert, *Phys. Rev. B* 1999, **59**, 1758-1775.
39. J. P. Perdew, Burke, K.; and Ernzerhof, M. *Phys. Rev. Lett*. 1996, **77**, 3865-3868.
40. M. Bahrami, J. Kieffer, H. Hashemi, X. Ma, R. M. Laine to be submitted.
41. Furgal J. C., T. Goodson III, R. M. Laine, "Synthesis of Decaphenyl Silsesquioxane (T_{10}) by Fluoride Catalyzed Rearrangement of $[PhSiO_{1.5}]_n$ and Phenyltri-ethoxysilane: Steady-State Spectroscopy and Larger Cages," to be submitted.
42. M. F. Roll, J. W. Kampf, Y. Kim, E. Yi, R. M. Laine, *J. Am. Chem. Soc*. 2010, **132**, 10171–10183.
43. R. M. Laine, S. Sulaiman, C. Brick, M. Roll, R. Tamaki, M. Z. Asuncion, M. Neurock, J. S. Filhol, C.Y. Lee, J. Zhang, T. Goodson III, M. Ronchi M. Pizzotti, S. C. Rand, Y. Li, *J. Am. Chem. Soc*. 2010, **132**, 3708–3722.
44. S. Sulaiman, J. Zhang, T. Goodson, III, R. M. Laine, *J. Chem. Mater*. 2011, **21**, 11177-11187.

Table of Contents Graphic